J. Fluid Mech. (1994), *vol.* 258, *pp.* 167–190

The effect of hydrodynamic interactions on the tracer and gradient diffusion of integral membrane proteins in lipid bilayers

By STUART J. BUSSELL, DANIEL A. HAMMER AND DONALD L. KOCH

School of Chemical Engineering, Cornell University, Ithaca, NY 14853, USA

(Received 2 October 1992 and in revised form 24 June 1993)

Biological membranes can be considered two-dimensional fluids with suspended integral membrane proteins (IMPs). We have calculated the effect of hydrodynamic interactions on the various diffusion coefficients of IMPs in lipid bilayers. The IMPs are modelled as hard cylinders of radius a immersed in a thin sheet of viscosity μ and thickness h bounded by a fluid of low viscosity μ'. We have ensemble averaged the N-body Stokes equations to the pair level and have renormalized them following the methods of Batchelor (1972) and Hinch (1977). The lengthscale for the hydrodynamic interactions is $\lambda a = \mu h/\mu'$, which is $O(100a)$, and the slow decay of the interactions introduces new features in the renormalizations compared to the analogous analyses for three-dimensional suspensions of spheres.

We have calculated the asymptotic limits for the short- and long-time tracer diffusivities, D_s and D_l, respectively, and for the gradient diffusivity, D_g, for $\phi \ll 1$ and $\lambda \gg 1$,where ϕ is the IMP area fraction and $\lambda = \mu h/(\mu' a)$. The diffusivities are

$$D_s/D_0 = 1-2\phi[1-(1+\ln(2)-9/32)/(\ln(\lambda)-\gamma)],$$
$$D_l/D_0 = D_s/D_0-0.07/(\ln(\lambda)-\gamma),$$
$$D_g/D_0 = 1+\phi[-7+(6\ln(2)+7/16+0.37)/(\ln(\lambda)-\gamma)],$$

where D_0 is the diffusivity in the limit of zero area fraction, and $\gamma = 0.577216$ is Euler's constant. The results for D_l and D_s differ only slightly. The decrease in D_g/D_0 as ϕ increases contrasts with the result for spheres for which $D_g/D_0 > 1$.

1. Introduction

Biological membranes of eucaryotic cells are fluid suspensions which consist of integral membrane proteins (IMPs) suspended in lipid bilayers (see figure 1; Singer & Nicholson 1972). Saffman (1976) calculated the diffusivity of a single IMP in a lipid bilayer based on a physical model that represents the proteins as cylinders of radius a immersed in a viscous sheet of viscosity μ and height h that is bounded by low-viscosity aqueous phases of viscosity μ'. This one-particle solution yields diffusivities that agree with measured values of the diffusivities of IMPs at very small IMP concentrations (Peters & Cherry 1982).

However, it is observed that the IMP diffusivities decrease substantially with increasing concentration. All previous theoretical descriptions of the effects of protein interactions on IMP diffusion have considered the hindering effects of the IMP's excluded area but have neglected hydrodynamic interactions (Abney, Scalettar & Owicki 1989*a*). The theoretical predictions of IMP diffusivities resulting from these

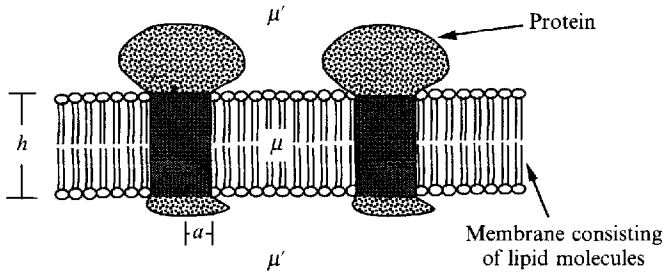

FIGURE 1. Cross-section of a typical biological membrane containing proteins and lipid molecules. The protein molecules have two regimes: a cylindrical core passing through the membrane and globular portions residing in the surrounding aqueous fluid.

purely thermodynamic theories are typically a factor of 2 or 4 higher than experimental measurements at high IMP area fractions, ϕ (Abney, Scalettar & Owicki 1989*a*; Peters & Cherry 1982; Chazotte & Hackenbrock 1988).

Since hydrodynamic interactions typically decrease the diffusivities (Batchelor 1976; Batchelor 1983; Brady & Bossis 1988), it is possible that hydrodynamic interactions can account for the lower diffusivities observed in experiments. As a first step toward understanding the effects of hydrodynamic interactions on the diffusion of integral membrane proteins, we shall derive short- and long-time tracer diffusion coefficients and the gradient diffusion coefficient in a dilute, monodisperse suspension of IMPs correct to $O(\phi)$.

The derivation will rely upon our previous calculation of the mobility functions for a pair of interacting IMPs (Bussell, Koch & Hammer 1992). The two-particle mobility calculation, like the one-particle analysis of Saffman (1976), involved a solution of the following two-dimensional equations for the membrane

$$\mu\nabla^2\boldsymbol{u} - \nabla p + 2\boldsymbol{\sigma}/h = 0, \tag{1}$$

$$\nabla\cdot\boldsymbol{u} = 0, \tag{2}$$

where μ, $\boldsymbol{u}$, p and h are the viscosity, velocity, pressure and height of the membrane and $\boldsymbol{\sigma}$ is the force per unit area that the aqueous phase exerts on the membrane. The velocity $\boldsymbol{u}$ is restricted to the plane of the membrane, because a large thermodynamic force resulting from the hydrophilic nature of the lipid head groups and the hydrophobic nature of the lipid tails confines them to the bilayer. The stress acting on the membrane is given by

$$\boldsymbol{\sigma} = \boldsymbol{n}\cdot(-p'\boldsymbol{I} + 2\mu'\boldsymbol{E})]_{z=0}, \tag{3}$$

where $\boldsymbol{E}' = \frac{1}{2}(\nabla\boldsymbol{u}' + \nabla\boldsymbol{u}'^{\dagger})$, $\boldsymbol{u}'$, p', and μ' are the rate of strain, velocity, pressure, and viscosity in the three-dimensional aqueous phase and $\boldsymbol{n}$ is the unit normal to the membrane. The equations of motion for the aqueous phase are the three-dimensional Stokes equations

$$\mu'\nabla^2\boldsymbol{u}' - \nabla p' = 0, \tag{4}$$

$$\nabla\cdot\boldsymbol{u}' = 0, \tag{5}$$

in the half-plane $z > 0$ with no-slip boundary conditions,

$$\boldsymbol{u}'|_{z=0} = \boldsymbol{u}. \tag{6}$$

Solutions of equations (1)–(6) may be obtained through an asymptotic analysis in a large parameter $\lambda = \mu h/(\mu' a)$, which is typically 100–1000 in biological applications. The singular perturbation analysis for $\lambda \gg 1$, yields a solution in an inner region,

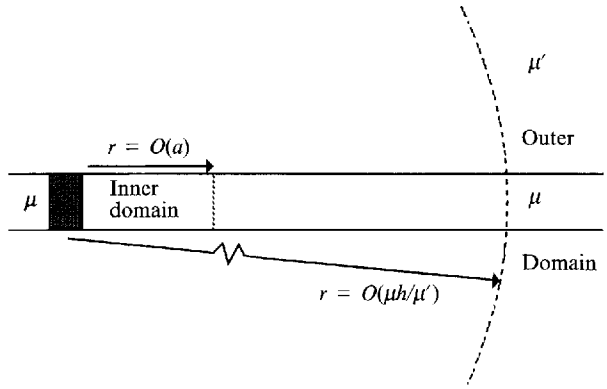

FIGURE 2. Membrane cross-section showing inner and outer domains. The inner domain includes only the membrane, while the outer domain includes all phases. Within the intermediate domain both the inner and outer solutions are valid.

corresponding to separations r from a protein for which $r \ll a\lambda$ and an outer region for which $r \gg a$ (see figure 2). In the inner solution the stress due to the aqueous phase may be neglected in (1), and (1) and (2) reduce to the two-dimensional Stokes equations. The inner solution for the velocity field produced by translation of an IMP behaves like $\ln(r)$ for $\lambda a \gg r \gg a$ and must be matched to an outer solution, which takes account of the stress in the aqueous phase.

At a separation $r = O(a\lambda)$, the drag exerted by the aqueous phase, $2\sigma/h = O(\mu' u/r)$, becomes comparable with the $O(\mu u/r^2)$ divergence of the membrane stress and all three terms must be retained in (1). However, the solution in the outer region is simplified because the IMPs may be treated as point forces exerted on the membrane fluid. Owing to the stress exerted on the three-dimensional fluid, the velocity produced by translation of an IMP decays like $1/r$ for $r \gg a\lambda$.

The two-particle solution was obtained by considering a near-field regime, in which the separation of the two proteins is $O(a)$ and both lie within the inner region, and a far-field regime, in which the separation is $O(\lambda a)$ and the hydrodynamic interactions may be treated using a point particle approximation (Bussell *et al.* 1992).

The tracer diffusion coefficients can be determined from the solutions of hydrodynamic problems in which an effective thermodynamic driving force is exerted on the tracer particle (Batchelor 1976, 1983). The short-time tracer diffusivity, D_s, applies for timescales $t \ll a^2/D_s$, for which no significant change of the configuration of the particle occurs.

In order to determine the effect of hydrodynamic interactions on the mobility of an IMP in a dilute monodisperse suspension, we ensemble average the hydrodynamic interactions based on the solution to the two-particle problem. The mobility, $\boldsymbol{m}$, is defined by

$$\boldsymbol{U} = \boldsymbol{f} \cdot \boldsymbol{m}, \tag{7}$$

where $\boldsymbol{U}$ is velocity and $\boldsymbol{f}$ is force. The mobilities of IMPs have unique values depending upon the environments in which they move. Tracer and gradient diffusion occur in distinct environments, and the natures of the driving forces differ. IMPs undergo tracer diffusion in macroscopically homogeneous environments. They experience random Brownian forces as a result of the thermal energy, kT, of the solvent, and their motions are undirected and uncorrelated. As a result, tracer diffusion coefficients are directly proportional to IMP mobilities when proteins are free of average net forces (Batchelor 1976, 1983).

Tracer diffusion coefficients of IMPs depend on the timescale over which the diffusion occurs. For times $t \ll a^2/D$, where D is the scalar diffusivity, particles travel short distances compared to a, and their relative positions in the suspension remain nearly unchanged. Since particle distributions do not change appreciably during this time interval, equilibrium radial-distribution functions are appropriate for the particle positions, and the diffusivities displayed are short-time diffusivities. Thus, the short-time diffusivity, D_s, is

$$\boldsymbol{D}_s = D_s \boldsymbol{I} = kT\boldsymbol{m}_s, \tag{8}$$

where $\boldsymbol{m}_s = m_s \boldsymbol{I}$ is the mobility relating the velocity of a protein to the force exerted on it, when the surrounding proteins are force- and torque-free and their positions are distributed according to the equilibrium distribution functions.

For longer time intervals, the relative positions of the particles change, and, when $t \gg a^2/D$, the growth of the mean-square displacement of a tracer particle is governed by the long-time tracer diffusion coefficient, D_l. Batchelor (1976) showed that the long-time diffusivity could be obtained from an equation of the form:

$$\boldsymbol{D}_l = D_l \boldsymbol{I} = kTm_l \boldsymbol{I}, \tag{9}$$

where m_l is the mobility relating the velocity of a tracer particle to an effective thermodynamic driving force acting upon it when the surrounding particles are force- and torque-free. In contrast to the calculation of the short-time mobility, the force acting on the particle in the calculation of m_l is maintained over a long time interval and the structure of the surrounding suspension is allowed to evolve in response to the motion of the tracer particle. Typical values for proteins in lipid bilayers are $D \sim 10^{-8}$ cm^2/s and $a \sim 2$ nm, so $a^2/D \sim O(10^{-6}$ s).

In contrast to the motions of IMPs in homogeneous environments, the motions of IMPs in concentration fields are directed and correlated. The diffusion coefficients relate the fluxes of the IMPs to the thermodynamic driving forces acting on each of the particles as a result of their concentration gradient. If we assume that the concentration fields obey the relation $L|\nabla \ln n| \ll 1$, all particles in an L^2 neighbourhood experience the same thermodynamic driving force, where L^2 is an area containing many particles and n is the number density of IMPs (Batchelor 1976). Diffusion coefficients of IMPs are accordingly directly proportional to the mobility, m_g, obtained when all proteins experience the same driving force,

$$\boldsymbol{D}_g \cdot \nabla n = nf^* m_g, \tag{10}$$

where $\boldsymbol{f}^*$ is the thermodynamic driving force. No relative motions occur between pairs of equal particles when they experience equal forces, so there is no perturbation to the equilibrium pair distribution. The hydrodynamic problem that must be solved to determine the gradient diffusivity for a monodisperse suspension is the same as the problem for a sedimenting suspension (Batchelor 1976).

Solutions of the ensemble-averaged Stokes equations for the mobilities of IMPs in membrane suspensions differ from the corresponding ones for spheres in three-dimensional suspensions because of the differing functionalities for the hydrodynamic interactions. The slowest decaying hydrodynamic interactions between spheres scale as $O(1/\rho)$, where $\rho = r/a$. For $\rho = O(1)$, the hydrodynamic interactions between IMPs scale as $O(\ln \rho)$ and therefore do not decay. The solutions for the mobilities of spheres (Batchelor 1976, 1982, 1983; Hinch 1977) involve renormalized forms of the ensemble-averaged Stokes equations. In this paper, mobilities of IMPs are found using the same methods as Batchelor and Hinch. Each IMP is interacting with all of its

neighbours within an $O(a\lambda)$ distance from its centre. Thus many ($O(\phi\lambda^2)$) proteins interact with each protein when $\lambda^{-2} \ll \phi \ll 1$. However, these long-range interactions are adequately described by an effective medium, which includes a renormalized viscosity. The renormalization of the viscosity was not required in Batchelor's studies of diffusion of spheres, because of the faster decay of the interactions in three dimensions (Batchelor 1976, 1982, 1983).

In §2, we discuss the ensemble-averaging techniques and identify the divergent pairwise IMP interactions which arise in the formulation. In §3, we follow the formalism developed by Batchelor (1976, 1982, 1983) and Hinch (1977) to renormalize the slowly decaying two-particle hydrodynamic interactions appearing in the ensemble-averaged Stokes equation in order to calculate D_s. We proceed to calculate D_l (Batchelor 1983) by solving for perturbations to the equilibrium distribution densities of IMPs caused by the motion of the tracer particle. In §4, we use the same ensemble-averaging and renormalization techniques to calculate gradient diffusivities of IMPs. Throughout the calculations, consideration is limited to monodisperse suspensions with hard disk potential interactions. These calculations result in the rigorously valid solutions for D_s, D_l, and D_g in the limit of low area fractions.

2. General methods

The methods we use are based on ensemble averages of hydrodynamic interactions (Hinch 1977). The membranes are treated as incompressible Newtonian fluids and the IMPs are approximated as hard disks with no-slip boundary conditions. The relevance of this simple model to a biological membrane is discussed by Saffman (1976) and Bussell *et al.* (1992). We begin our formal analysis of the suspension by considering the N-body equation of momentum conservation for the membrane,

$$\nabla \cdot \boldsymbol{T}(\boldsymbol{x} \mid \chi) = -\boldsymbol{f}(\boldsymbol{x} \mid \chi) - \frac{2\boldsymbol{\sigma}}{h}, \tag{11}$$

where $\boldsymbol{T}$ is the stress tensor, $\boldsymbol{x}$ is a position in the suspension, χ is the configuration of the N-particles in the suspension with particle q, $q = 1$ to N, centred at $\boldsymbol{x}_q$, $\boldsymbol{f}$ represents the thermodynamic driving forces applied to the proteins and $\boldsymbol{\sigma}$ is the stress exerted by the aqueous phase. The stress tensor in the membrane is

$$\boldsymbol{T} = -p(\boldsymbol{x} \mid \chi)\boldsymbol{I} + 2\mu \boldsymbol{E}(\boldsymbol{x} \mid \chi) + \boldsymbol{T}^p(\boldsymbol{x} \mid \chi), \tag{12}$$

where p is pressure, μ is the viscosity of the membrane, $\boldsymbol{E}$ is the Eulerian rate of strain tensor, and $\boldsymbol{T}^p$ is a generalized function which represents the extra stress above the value specified by the fluid law if $\boldsymbol{x}$ is inside any particle and is zero otherwise. The Eulerian rate of strain tensor is

$$\boldsymbol{E}(\boldsymbol{x} \mid \chi) = \tfrac{1}{2}(\nabla \boldsymbol{u}(\boldsymbol{x} \mid \chi) + (\nabla \boldsymbol{u}(\boldsymbol{x} \mid \chi))^t), \tag{13}$$

where $\boldsymbol{u}$ is velocity. Along with Stokes equation, there is also the continuity equation,

$$\nabla \cdot \boldsymbol{u}(\boldsymbol{x} \mid \chi) = 0. \tag{14}$$

There is a hierarchy of ensemble averages of the N-body equation conditioned on the location of q particles, $q = 0$ to N. This hierarchy may be truncated and solved at the q level, generating errors of $O(\phi^{q+1})$ and higher, provided that they are properly first renormalized. Ensemble averages of functions involve integrations over the positions of specified particles, and integration over the position of a particle reduces the number of particles that the function depends upon by one.

We make use of a variety of distribution functions, and the following examples establish the normalization convention,

$$\left.\begin{aligned} 1 &= \int P(\chi)\,\mathrm{d}x_1\,\mathrm{d}x_2\ldots\mathrm{d}x_N, \\ P_2(x_1,x_2) &= N(N-1)\int P(\chi)\,\mathrm{d}x_3\,\mathrm{d}x_4\ldots\mathrm{d}x_N, \\ P_2(x_2\,|\,x_1) &= \frac{P_2(x_1,x_2)}{P_1(x_1)} = \frac{V}{N}P_2(x_1,x_2) = \frac{1}{n}P_2(x_1,x_2), \end{aligned}\right\} \tag{15}$$

where all particles are indistinguishable. $P(\chi)$ is the probability density function of the N-body configuration χ, $P_2(x_2,x_1)$ is the probability density function for any particle pair at positions x_1 and x_2, and $P_2(x_2\,|\,x_1)$ is the probability density function of a particle at x_2 conditioned on a particle at x_1. In future equations, we omit the subscript on probability density functions because their arguments suffice to indicate the number of particles involved.

The $q = 0$ equations are

$$\nabla\cdot\langle\boldsymbol{T}\rangle(x) = -\langle f\rangle(x) - \frac{2\langle\sigma\rangle}{h}, \tag{16}$$

$$\langle\boldsymbol{T}\rangle(x) = -\langle p\rangle(x)\boldsymbol{I} + 2\mu\langle\boldsymbol{E}\rangle(x) + \langle\boldsymbol{T}^p\rangle(x), \tag{17}$$

$$\langle\boldsymbol{T}^p\rangle(x) = \int_{|x-x_1|\leqslant a}\langle\boldsymbol{T}^p\rangle(x\,|\,x_1)\,P(x_1)\,\mathrm{d}V_1, \tag{18}$$

$$\nabla\cdot\langle u\rangle(x) = 0, \tag{19}$$

where the $\langle\ \rangle$ symbols indicate an ensemble average. Notice that the $q = 0$ ensemble-averaged equations involve the $q = 1$ conditionally averaged extra stress, $\langle\boldsymbol{T}^p\rangle(x\,|\,x_1)$. The solution of the $q = 0$ equations requires data for the $q = 1$ equations or an approximation.

The one-particle conditionally averaged equations, $q = 1$, are similar to the $q = 0$ equation,

$$\nabla\cdot\langle\boldsymbol{T}\rangle(x\,|\,x_1) = -\langle f\rangle(x\,|\,x_1) - \frac{2\langle\sigma\rangle}{h}, \tag{20}$$

$$\langle\boldsymbol{T}\rangle(x\,|\,x_1) = -\langle p\rangle(x\,|\,x_1)\boldsymbol{I} + 2\mu\langle\boldsymbol{E}\rangle(x\,|\,x_1) + \langle\boldsymbol{T}^p\rangle(x\,|\,x_1), \tag{21}$$

$$\langle\boldsymbol{T}^p\rangle(x\,|\,x_1) = \int_{|x-x_1|\leqslant a}\langle\boldsymbol{T}^p\rangle(x\,|\,x_1,x_2)\,P(x_2\,|\,x_1)\,\mathrm{d}V_1, \tag{22}$$

$$\nabla\cdot\langle u\rangle(x\,|\,x_1) = 0. \tag{23}$$

At this level, the highest-order effects involve two-body interactions via the $\langle\boldsymbol{T}^p\rangle(x\,|\,x_1,x_2)$ term in (22). This is the highest level at which we calculate the mobility and diffusivity of IMPs. Extending the calculations to higher order requires results for three-body interactions. However, simulation techniques might be best suited to evaluate suspension behaviour at the level of detail involving three-body interactions or higher (Brady & Bossis 1988).

The ensemble averaging of the equations of motion for the three-dimensional fluid, (4) and (5), and the boundary conditions linking the three- and two-dimensional fluids,

(3) and (6), present no special problems since these equations are linear and the three-dimensional fluid contains no particles. The results are:

$$\langle \boldsymbol{\sigma} \rangle (\boldsymbol{x} \,|\, \boldsymbol{x}_1) = \boldsymbol{n} \cdot (-\langle p' \rangle (\boldsymbol{x} \,|\, \boldsymbol{x}_1)) \boldsymbol{I} + 2\mu \langle \boldsymbol{E}' \rangle (\boldsymbol{x} \,|\, \boldsymbol{x}_1)|_{z=0}, \tag{24}$$

$$\mu' \nabla^2 \langle \boldsymbol{u}' \rangle (\boldsymbol{x} \,|\, \boldsymbol{x}_1) - \nabla \langle p' \rangle (\boldsymbol{x} \,|\, \boldsymbol{x}_1) = 0, \tag{25}$$

$$\nabla \cdot \langle \boldsymbol{u}' \rangle (\boldsymbol{x} \,|\, \boldsymbol{x}_1) = 0, \tag{26}$$

$$\langle \boldsymbol{u}' \rangle (\boldsymbol{x} \,|\, \boldsymbol{x}_1)|_{z=0} = \langle \boldsymbol{u} \rangle (\boldsymbol{x} \,|\, \boldsymbol{x}_1). \tag{27}$$

We solve the one-particle conditionally averaged equations, (20)–(23), in the inner region where the stress $2\langle \boldsymbol{\sigma} \rangle / h$ in (20) can be neglected by inverting them using a Green function technique. This operation involves the approximation of pairwise additive particle interactions. The technique of ensemble averaging is complicated because quantities determined by pairwise addition of interactions diverge as the averaging domain increases. This divergence necessitates renormalizing the problem (Hinch 1977). Renormalization of the ensemble-averaged equations involves treating the slowest decaying particle interactions in terms of an effective medium, so as to avoid the divergent pairwise summation.

We use the method of reflections to identify the slowly decaying interactions which diverge when added pairwise (Kim & Karrila 1991). The method of reflections approximates fluid dynamic solutions by successively evaluating disturbances caused by particle interactions. Each disturbance creates new responses and, hence, the method is iterative. The velocities and forces of a particle are repeatedly related to external flow fields using Faxén laws.

The formulation of the renormalization procedure for $\rho \ll \lambda$ involves the two-dimensional analogue of the Oseen–Burgers tensor, and its derivatives, which is the Green function for the two-dimensional Stokes equation. The Oseen–Burgers tensor characterizes the creeping flow response of a three-dimensional Newtonian fluid to a point-force. The two-dimensional analogue is found by solving for the flow field which results from a force applied to an isolated disk and taking the limit as the disk radius goes to zero (Kim & Karrila 1991). The two-dimensional Oseen–Burgers tensor is

$$\boldsymbol{J}(z) = \frac{1}{4\pi\mu} \left[\frac{z_i z_j}{z^2} - \ln\left(\frac{z}{a}\right) \boldsymbol{\delta}_{ij} - \tfrac{1}{2} \boldsymbol{\delta}_{ij} \right]. \tag{28}$$

There is an arbitrary isotropic term in (28), and we find it convenient to put the $\ln(a)$ term in the tensor. The arbitrary term arises because the velocity of a disk undergoing Stokes flow in response to a force in a two-dimensional fluid is indeterminate.

We use the two-dimensional Oseen–Burgers tensor, along with the appropriate Faxén laws, to identify the strength of the reflections arising from particle interactions. The Faxén laws relate the motions of a particle to their force moments and an imposed velocity field. They are derived by using the reciprocal theorem (Kim & Karrila 1991). The relevant Faxén laws for a two-dimensional fluid are

$$\boldsymbol{U} = f m_0 + (1 + \tfrac{1}{4} a^2 \nabla^2) \boldsymbol{v}_\infty, \tag{29}$$

$$\boldsymbol{S} = 4\pi\mu a^2 (1 + \tfrac{1}{8} a^2 \nabla^2) \boldsymbol{E}_\infty, \tag{30}$$

where $\boldsymbol{U}$ is the velocity of a particle, m_0 is its mobility as an isolated particle, $\boldsymbol{v}_\infty$ is the external velocity field, $\boldsymbol{S}$ is the stresslet of a particle, and $\boldsymbol{E}_\infty$ is the external rate of strain. The mobility of an isolated particle in a membrane is (Saffman 1976)

$$m_0 = \frac{[\ln(\lambda) - \gamma]}{4\pi\mu h}. \tag{31}$$

In deriving (29), it is necessary to apply the reciprocal theorem to a region bounded by the particle surface and a surface at a separation in the matching region, i.e. $a \ll r \ll a\lambda$. Thus, the factor fm_0 in (29) arises from the matching of the inner solution considered here to an outer solution that includes the effect of the surrounding aqueous phases.

The external velocity field in two dimensions is slightly different from the equivalent quantity in a three-dimensional fluid. It has the value

$$\boldsymbol{v}_\infty = \int (\boldsymbol{f}^{(n)} m_0 + \boldsymbol{f}^{(n)} \cdot \boldsymbol{J}(\boldsymbol{x} - \boldsymbol{y}^{(n)}))\, w^{(n)}\, \mathrm{d}V, \tag{32}$$

where $\boldsymbol{f}^{(n)}$ are external point-forces of strength $w^{(n)}$ at locations $\boldsymbol{y}^{(n)}$. The $\boldsymbol{f}^{(n)} m_0$ terms in the integral again arises because of the divergent nature of the two-dimensional Oseen–Burgers tensor. It represents the velocity at $\boldsymbol{y}^{(n)}$ from a point-force there and again is only determined after matching to an outer solution.

Using the two-dimensional Oseen–Burgers tensor and the Faxén laws, we may determine the strength of the reflection terms which affect the velocity of particles undergoing tracer or gradient diffusion. Since we are integrating the two-particle interactions over all relative positions, any terms which decay like $O(r^{-2})$ or slower cause a divergence when inverting the ensemble-average equations, (20)–(23), where now $r = |\boldsymbol{x} - \boldsymbol{x}_1|$.

The zeroth-order solution for the velocity field resulting from a force on a central particle, $\boldsymbol{f}$, is the solution for the velocity resulting from a force on an isolated disk,

$$^{(0)}\boldsymbol{u} = {}^{(0)}U + (\boldsymbol{J} + \tfrac{1}{4}a^2\nabla^2\boldsymbol{J}) \cdot \boldsymbol{f}, \tag{33}$$

where $^{(0)}\boldsymbol{u}$ is the zeroth-order velocity disturbance, $^{(0)}U$ is the zeroth-order velocity of the protein, and $\boldsymbol{f}$ is also the force the protein exerts on the surrounding fluid. Looking at the velocity disturbance, we see that a forced particle creates a velocity disturbance with a force term, $\boldsymbol{J} \cdot \boldsymbol{f}$, which is $O(\ln(r))$, and a quadrupole term, $\nabla^2 \boldsymbol{J} \cdot \boldsymbol{f}$, which is $O(r^{-2})$.

Based on (29) and (33) and setting $\boldsymbol{v}_\infty = {}^{(0)}\boldsymbol{u}$, the first-order disturbance to the velocity of an IMP neighbouring the central particle, $^{(1)}U$, is, to leading order, $^{(0)}\boldsymbol{u}$ evaluated at a separation distance of r or $O(\ln(r)) + O(r^{-2})$. The term $^{(1)}fm_0$ in (17) is zero because the forces on all proteins are set by the boundary conditions and, thus, only zeroth-order forces can be non-zero. The stresslets of neighbouring IMPs are the lowest-order poles affected by the velocity disturbance because the torques are also set by the boundary conditions. Based on (18), the first-order stresslet, $^{(1)}\boldsymbol{S}$, of neighbouring particles resulting from $^{(0)}\boldsymbol{u}$ are proportional to $\nabla(^{(0)}\boldsymbol{u})$ which is the sum of an $O(r^{-1})$ term and a non-divergent $O(r^{-3})$ term. These stresslets then induce first-order velocity disturbances, $^{(1)}\boldsymbol{u}$, equal to $^{(1)}\boldsymbol{S} \cdot O(r^{-1})$ or $O(r^{-2})$. The $O(r^{-1})$ factor is the strength of a dipole-driven velocity field. The first-order velocity disturbances generated by neighbouring proteins create a second-order disturbance to the velocity of the central protein, $^{(2)}U$, equal to $^{(1)}\boldsymbol{u}|_r$ or $O(r^{-2})$. Higher reflections decay faster by $O(r^{-2})$ relative to the previous reflection.

This procedure allows us to identify terms which require renormalization in both the tracer and gradient diffusion problems. The first-order disturbance to the velocity of a tracer protein, $^{(1)}U$, is zero because neighbouring proteins are force-free and create no zeroth-order velocity disturbances. Hence, the velocity of a forced particle in the tracer diffusion problem has a divergence like $\int {}^{(2)}U r\, \mathrm{d}r$ or $O(\ln(r))$. This result contrasts with the sphere problem for which the integrals arising from the inversion of the ensemble-averaged equations for the velocity of a tracer particle in a suspension are absolutely convergent (Aguirre & Murphy 1973; Batchelor 1976).

In contrast to the tracer diffusion problem which has only one term which decays slower than $O(r^{-2})$, the gradient diffusion problem has three terms which require renormalization. The calculation for the mobility of a central particle undergoing gradient diffusion involves the same divergent pairwise term as a tracer particle. In addition, it also involves divergent terms caused by the first-order disturbances to the central particle's velocity, ${}^{(1)}\boldsymbol{U}$. This disturbance is caused by its neighbouring particles which experience the same thermodynamic forces driving the central particle. Based on this identification of divergent terms, we renormalize the tracer and gradient diffusivity problems following the methods of Hinch (1977) and Batchelor (1972).

Three-particle interactions are neglected because they make $O(\phi^2)$ corrections to the diffusivities. The effect of the slowest decaying reflection involving three particles on the velocity of the test particle decays like $r_{12}^{-1} r_{23}^{-2} r_{31}^{-1}$, where r_{ij} is the separation between particles i and j and the test particle is particle 1. Averaging over the positions of particles 2 and 3 leads to a logarithmically divergent integral, similar to that obtained in the two-particle problem. However, this divergence can be removed (as before) by renormalizing the viscosity to the next order in the area fraction expansion.

3. Tracer diffusion

3.1. *Short-time diffusivity*

We solve a renormalized version of the one-particle conditionally averaged Stokes equations to determine the short-time diffusivity, $\boldsymbol{D}_s$, of the tracer IMP in the presence of force-free IMPs. At the limit of low ϕ, the pair probability, $P(\boldsymbol{x}_2|\boldsymbol{x}_1)$, is uniform throughout the suspension. The mobilities of particles experiencing either a Brownian or constant force are identical, and they are related to short-time diffusion coefficients by (8).

We define the velocity of an IMP resulting from a force as $\langle \boldsymbol{u} \rangle(\boldsymbol{x}|\boldsymbol{x}_1) - \langle \boldsymbol{u} \rangle(\boldsymbol{x})$. Unless the suspension as a whole experiences a net force, the unconditionally averaged velocity of the suspension, $\langle \boldsymbol{u} \rangle(\boldsymbol{x})$, is zero.

At the lowest level of approximation, the suspension is a pure lipid bilayer and contains no tracer particles. At the next level, the suspension contains an isolated protein in an infinite medium. The solution for the particle mobility is given by (31). The next level of approximation incorporates the first effects of particle interactions. The two-particle hydrodynamic interactions are correctly represented to $O(1)$ by the solution of two isolated particles in an infinite medium (Bussell *et al.* 1992). Given a configuration for two particles, there is an $O(\phi)$ correction to the hydrodynamics caused by the presence of other particles. As mentioned earlier, solution of (20)–(23) by simple inversion with the pure fluid Green function results in non-convergent solutions. Thus, we must renormalize the equations, and this involves determining the bulk properties of the membrane to $O(\phi)$ (Hinch 1977).

The bulk properties of a membrane in response to the motion of a tracer protein are characterized by the response of force-free proteins to the flow-field generated by the tracer particle. The force-free proteins respond with a velocity field driven by a stresslet. Determining the bulk stress tensor in the membrane to $O(\phi)$ is analogous to finding the Einstein viscosity for a suspension of spheres (Einstein 1905) and this calculation has been performed for a suspension of n-dimensional particles by Brady (1984). The equivalent of the Einstein viscosity in a two-dimensional fluid is therefore,

$$\bar{\mu} = (1 + 2\phi)\mu. \tag{34}$$

The governing equations, (20)–(23), for the velocity of a tracer protein are

renormalized using the effective viscosity. The renormalized one-particle conditional equation for the velocity of a tracer particle resulting from a force is derived by inserting (21) and (22) into (20) and incorporating the change in divergence of the stress associated with the effective viscosity into both sides of the equation. The result is, for $r \geqslant a$,

$$-\nabla\langle p\rangle(x\,|\,x_1)+\nabla\cdot(2\mu^*\langle \boldsymbol{E}\rangle(x\,|\,x_1))+\frac{2}{h}\langle\boldsymbol{\sigma}\rangle(x\,|\,x_1)$$

$$=-\nabla\cdot\int_{|x_1-x_2|\geqslant 2a}[\langle \boldsymbol{T}^p\rangle(x\,|\,x_1,x_2)\,P(x_2\,|\,x_1)-4g(x_2\,|\,x_1)\,\phi\mu\langle \boldsymbol{E}\rangle(x_2\,|\,x_1)\,\delta(x-x_2)]\,\mathrm{d}V_2, \tag{35}$$

where x_1 is now located at the centre of the tracer particle,

$$\mu^*=\begin{cases}\mu & \text{for } a<|x_2-x_1|<2a,\\ \mu_{eff}=(1+2g(x_2\,|\,x_1)\,\phi)\,\mu & \text{for } 2a<|x_2-x_1|,\end{cases} \tag{36}$$

and g is the radial distribution function. The radial distribution function is necessary in order to extend the formulation to cases in which the pair distribution function, $P(x_2\,|\,x_1)$, is not uniform. The renormalization removes the divergent $O(r^{-2})$ term which affects ${}^{(2)}U$.

Equation (35) is most easily solved by expanding in a Taylor series in ϕ. The zeroth-order equation is taken as the complete left-hand side of (35) with the right-hand side set equal to zero,

$$-\nabla p^0(x\,|\,x_1)+\nabla\cdot(2\mu^*\boldsymbol{E}^0(x\,|\,x_1))+\frac{2\boldsymbol{\sigma}^0}{h}(x\,|\,x_1)=0. \tag{37}$$

The solution of (37) has an $O(1)$ contribution which is the solution for the velocity field driven by a forced disk in a pure lipid bilayer and an $O(\phi)$ contribution that arises from the effective viscosity. The $O(\phi)$ remainder to the solution of (35) is ϕ multiplied by the solution of

$$-\nabla p^1(x\,|\,x_1)+\nabla\cdot(2\mu\boldsymbol{E}^1(x\,|\,x_1))+\frac{2\boldsymbol{\sigma}^1(x\,|\,x_1)}{h}$$

$$=-\nabla\cdot\int_{|x_1-x_2|\geqslant 2a}[\langle \boldsymbol{T}^{p''}\rangle(x\,|\,x_1,x_2)\,g(x_2\,|\,x_1)-4g(x_2\,|\,x_1)\,\mu\boldsymbol{E}''(x_2\,|\,x_1)\,\delta(x-x_2)]\,\mathrm{d}V_2, \tag{38}$$

where $\boldsymbol{T}^{p''}$ and $\boldsymbol{E}''$ are the $O(1)$ results when particle 1 has a force and is in the presence of a single force-free particle in a lipid bilayer. Both $\boldsymbol{T}^{p''}$ and $\boldsymbol{E}''$ do not have to be evaluated in the effective medium because the $O(\phi)$ correction to the result from the effective viscosity leads to an $O(\phi^2)$ contribution to the remainder. The utility of this formulation is that (38) can be inverted and solved using the two-dimensional Oseen–Burgers tensor.

The velocity field generated by a forced protein moving through a fluid with viscosity μ for $a<|x_2-x_1|<2a$ and μ_{eff} for $2a<|x_2-x_1|$ is given by the solution to (37). The effective viscosity is a function of r if g is non-uniform. Equation (37) has two possible solution algorithms. The differential equation can be solved by discretizing the fluid for $2a<|x_2-x_1|$ in order to account for the non-constant viscosity. The equation is solved in l_{tot} discrete annular regions surrounding the tracer particle, where the viscosity is evaluated at the centre of each annulus. The stresses and velocities are set equal at the

boundaries between regions, and the resulting system of equations is solved numerically. On the other hand, (37) can be numerically integrated. We have chosen the first algorithm because it is analogous to the technique Hinch (1977) used for spheres at low ϕ. Within each region, (37) is the Stokes equation for the pure lipid bilayer. After solving the Stokes and continuity equations in each region and applying no-slip boundary conditions at the surface of the IMP, we find that the velocity field is

$$u_i = U_i + c_1^{(1)} f_j \left(\frac{x_j x_i}{r^2} - \ln\left(\frac{r}{a}\right)\delta_{ij} \right) + c_3^{(1)} f_j \left(\frac{-\delta_{ij}}{a^2} + \frac{-\delta_{ij}}{r^2} - \frac{2x_j x_i}{r^4} \right) + c_5^{(1)} f_j \left(-\tfrac{2}{3} x_j x_i + (r^2 - a^2)\delta_{ij} \right) \quad \text{for} \quad l = 1 (a < |\boldsymbol{x}_2 - \boldsymbol{x}_1| < 2a), \tag{39}$$

$$u_i = c_0^{(l)} U_i + c_1^{(l)} f_j \left(\frac{x_j x_i}{r^2} - \ln\left(\frac{r}{a}\right)\delta_{ij} \right) + c_3^{(l)} f_j \left(\frac{-\delta_{ij}}{a^2} + \frac{-\delta_{ij}}{r^2} - \frac{2x_j x_i}{r^4} \right) + c_5^{(l)} f_j \left(-\tfrac{2}{3} x_j x_i + (r^2 - a^2)\delta_{ij} \right) \quad \text{for} \quad 2 < l < l_{tot-1}, \tag{40}$$

$$u_i = c_6 U_i + c_7 J_{ij} f_j + c_8 \nabla^2 J_{ij} f_j \quad \text{for} \quad R_{trunc} < |\boldsymbol{x}_2 - \boldsymbol{x}_1|. \tag{41}$$

Equation (40) for l is valid for $|\boldsymbol{x}_2 - \boldsymbol{x}_1|$ such that, $(l-2) < (|\boldsymbol{x}_2 - \boldsymbol{x}_1| - 2a)(l_{tot} - 2)/(R_{trunc} - 2a) < (l-1)$, where R_{trunc} is the value of $|\boldsymbol{x}_2 - \boldsymbol{x}_1|$ at which we assume $g(|\boldsymbol{x}_2 - \boldsymbol{x}_1|) = 1$. In practice, it was the distance at which $|g(|\boldsymbol{x}_2 - \boldsymbol{x}_1|) - 1| < 0.04$. For all area fractions, $9.98a < R_{trunc} < 11.76a$. The U_i in (39) is the velocity of the tracer particle needed to solve for its mobility.

The constant terms are determined by equating the velocities and stresses at the boundaries separating the regions. This procedure is easily automated for the case in which the pair-probability has structure. In the limit $\phi \to 0$, the pair-probability is constant and only two regions are necessary. In this case the solution is

$$\left.\begin{aligned} c_1^{(0)} &= \frac{1}{4\pi\mu}, \\ c_3^{(0)} &= \frac{a^2\left(3\frac{\bar{\mu}}{\mu} + 5\right)}{(30\bar{\mu} + 34\mu)\pi}, \\ c_5^{(0)} &= \frac{9\left(\frac{\bar{\mu}}{\mu} - 1\right)}{4\pi a^2 (30\bar{\mu} + 34\mu)}, \\ c_7 &= 1, \\ c_8 &= \frac{a^2\left(-9\frac{\bar{\mu}}{\mu} + 17\right)}{\left(15\frac{\bar{\mu}}{\mu} + 17\right)}, \\ c_6 U_i &= U_i + \frac{f_i}{4\pi(15\bar{\mu} + 17\mu)}\left[9\left(\frac{\bar{\mu}}{\mu} - 1\right) - \ln(2)\left(15\frac{\bar{\mu}}{\mu} + 17\right)\right]. \end{aligned}\right\} \tag{42}$$

We determine the final unknown, U_i, by matching the inner solution with the outer solution for $a \ll |\boldsymbol{x}_2 - \boldsymbol{x}_1| \ll \lambda a$ obtained by solving (37) with (24)–(27) (Saffman 1976). After performing this match, we find

$$\boldsymbol{U} = \frac{\boldsymbol{f}}{4\pi\mu}\left\{\frac{1}{(1+2\phi)}\left[\ln(\lambda(1+2\phi)) - \gamma + 2\phi\left(\ln(2) - \frac{9(1+2\phi)}{15(1+2\phi)+17}\right)\right]\right\}. \tag{43}$$

The asymptotic value of (43) as $\phi \to 0$, expressed as a ratio of U_0, is

$$\frac{U}{U_0} = \frac{m_s}{m_0} = \frac{D_s}{D_0} = 1 - 2\phi\left[1 - \frac{1+\ln(2)-9/32}{\ln(\lambda)-\gamma}\right] + \text{remainder}. \tag{44}$$

For $\lambda = 250$, a typical value for IMP-membrane systems,

$$\frac{U}{U_0} = \frac{m_s}{m_0} = \frac{D_s}{D_0} = 1 - 1.43\phi + \text{remainder}. \tag{45}$$

Equations (44) and (45) give the results for the short-time diffusivity obtained by replacing the particles surrounding the tracer particle by an effective viscosity (36). The same result could have been obtained by replacing each of the neighbouring particles by a point dipole of strength $4\pi\mu a^2\langle \boldsymbol{E} \rangle(\boldsymbol{x}_2 \mid \boldsymbol{x}_1)$. Indeed, the renormalization leading to (35) is not strictly required for the problem of tracer diffusion in a membrane. The integration of the term $\langle \boldsymbol{T}^p \rangle(\boldsymbol{x} \mid \boldsymbol{x}_1, \boldsymbol{x}_2)\, \boldsymbol{P}(\boldsymbol{x}_2 \mid \boldsymbol{x}_1)\, \mathrm{d}V_2$ in (35) will converge and give the same result as (44) and (45) if the integration is carefully performed over both the inner and outer regions. However, the renormalized form of (35) has the advantage that the remainder term (given by (46) below) can be evaluated by integrating over the inner region only.

In addition, the renormalization leads to a physically appealing interpretation of the change of mobility in terms of the effects of a modified effective viscosity. The physical origin of the various terms in (44) may be interpreted as follows. There is a decrease, -2ϕ, in the ratio of the mobility to its value at infinite dilution, owing to the increased stress on the protein associated with the change in effective viscosity from μ to $\mu(1+2\phi)$. There is an increase, $2\phi/(\ln(\lambda)-\gamma)$, caused by the alteration of the outer solution and matching conditions associated with the increased viscosity of the membrane. Finally, there is an increase in the mobility ratio of $2\phi(\ln(2)-\frac{9}{32})/(\ln(\lambda)-\gamma)$ caused by the lower viscosity associated with the exclusion of particles from the region, $a < r < 2a$. It will be seen that the renormalization we have used, including a change in the viscosity owing to volumetric exclusion near the tracer particle, leads to quite accurate results even without the inclusion of the remainder term.

Equation (38) corrects for the higher multipole interactions neglected by the effective medium approximation. It is evaluated using the two-particle solutions of Bussell *et al.* (1992). After inversion of (38) with the pure solvent Green function, the solution for the $O(\phi)$ remainder to the velocity of particle 1 neglected by (37) is

$$\text{remainder} = \frac{1}{U_0^2}\int_{|\boldsymbol{x}_1-\boldsymbol{x}_2|\geqslant 2a} \boldsymbol{U}_0 \cdot [\boldsymbol{U}_2'' - 4\pi\mu a^2 \boldsymbol{E}''(\boldsymbol{x}_2 \mid \boldsymbol{x}_1) : \nabla \boldsymbol{J}(\boldsymbol{x}_2 - \boldsymbol{x}_1)]\, P(\boldsymbol{x}_2 \mid \boldsymbol{x}_1)\, \mathrm{d}V_2. \tag{46}$$

The velocity $\boldsymbol{U}_2''$ is the disturbance to the velocity of the tracer particle to $O(1)$ caused by the presence of a neighbouring particle. It is taken from the solution for two isolated particles and is

$$\boldsymbol{U}_2'' = \frac{\boldsymbol{f}}{\mu h} \cdot \left(\frac{a_m \boldsymbol{x}\boldsymbol{x}}{r^2} + c_m\left(\boldsymbol{I} - \frac{\boldsymbol{x}\boldsymbol{x}}{r^2}\right)\right) - \boldsymbol{f} m_0, \tag{47}$$

where a_m should not be confused with the particle radius: both a_m and c_m are components of the mobility matrix (Bussell *et al.*) which relates the velocities of the proteins to their forces. The second term in (46) arises from the renormalization. It contains the terms which contribute to the effective viscosity of the medium.

The rate of strain $\boldsymbol{E}''(\boldsymbol{x}_2 \mid \boldsymbol{x}_1)$ is evaluated with the $O(1)$ contribution to $\boldsymbol{u}^0$ which is the velocity disturbance emanating from an isolated IMP in a pure lipid bilayer, (33).

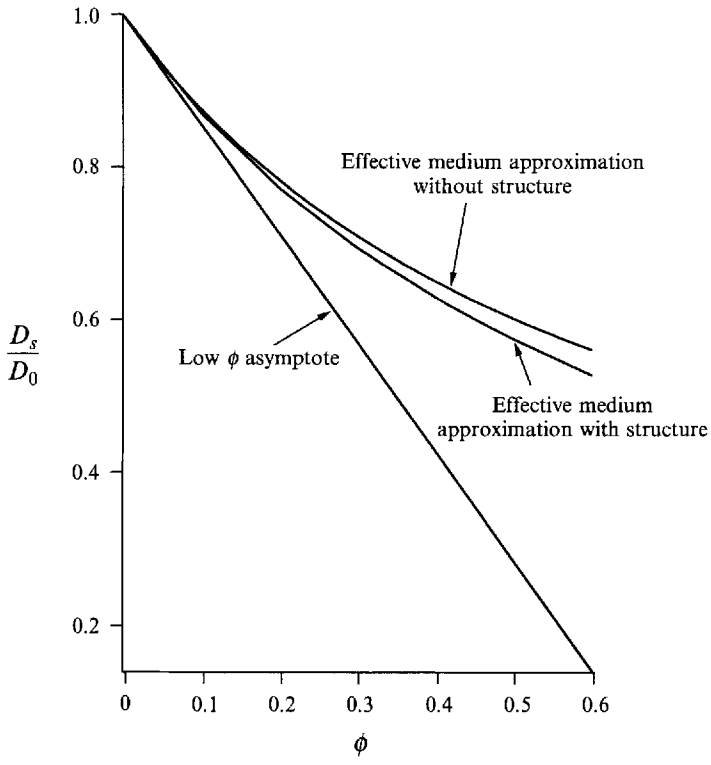

FIGURE 3. The normalized short-time diffusivity, D_s/D_0, for an IMP-membrane system with $\lambda = 250$. The full solution with structure incorporates non-uniform radial distribution functions based on hard disk interactions into the solutions. The full solutions have a nonlinear dependence on ϕ which exceeds the rigorous precision of the results which are limited to $O(\phi)$.

This is an approximation which is valid for results limited to $O(\phi)$. The evaluation of the integral in (46) completes the calculation for the tracer diffusivity at short times and low ϕ. In the limit as $\phi \to 0$, we find

$$\text{remainder} = \frac{8.35 \times 10^{-4}\phi}{\ln(\lambda) - \gamma}. \tag{48}$$

The remainder is small compared to (44), the effective medium approximation to the tracer velocity. The remainder continues to be insignificant at high ϕ. Recalling our discussion of the method of reflections, the integral in (46) converges like $\int {}^{(4)}U r\,\mathrm{d}r$ after removal of the ${}^{(2)}U$ reflection. Therefore, the rate of convergence is $O(r^{-3}\,\mathrm{d}r)$. As a result, we are justified in evaluating the particle interactions in $r < \lambda a$ and then matching to the outer solution.

Equations (44) and (48) give the asymptotic result for small volume fraction of the tracer diffusivity with errors of $O(\phi^2)$. The most reliable method for determining the diffusivity at higher volume fraction is through Stokesian dynamic simulations, such as those performed for the short-time diffusivity of spherical particles by Phillips *et al.* (1988). However, in figure 3, we present the results given by (43) over a range of volume fraction. Equation (43) represents an effective medium approximation in which the effect of the surrounding particles is represented by an effective viscosity (36) with the pair probability given by $g = 1$. This effective medium approximation is similar to one suggested by Beenaker & Mazur (1982; their equation (8.2)). In the case of spherical

particles, the exact calculations (Phillips *et al.* 1988; Beenaker & Mazur 1984) were found to lie between the low volume fraction asymptote and the effective medium approximation. We have also calculated the diffusivity of a particle in an effective medium given by (36) with the pair probability $g(\phi, r)$ obtained from a Monte Carlo simulation of a hard disk suspension at equilibrium (Metropolis *et al.* 1953; Chae, Ree & Ree 1969). Since the effective viscosity is now varying continuously in the region, $r > 2a$, equation (43) is no longer applicable. Instead, we solve (39), (40), and (41) for l_{tot} regions. We found that results with a precision of $\pm 0.1\%$ could be obtained by using 200 regions. A comparison of these results with those obtained from (43) (see figure 3) indicates that the structure of the pair probability has a small effect on the short-time diffusivity according to the effective medium approximation.

Unfortunately, we are unaware of any experimental data for short-time diffusion coefficients of IMPs large enough relative to the lipid molecules so that the hydrodynamic model is appropriate. Current techniques have a time resolution of $O(1\text{ s})$, which is far too slow for measuring D_s (Qian, Sheetz & Elson 1991).

3.2. *Long-time diffusivity*

Following Batchelor (1976, 1982), we derive the long-time diffusivity of a tracer particle by considering the average velocity in response to a small thermodynamic driving force. The motion produced by the driving force is small compared with the undirected Brownian motion (for small deviations from equilibrium) as expressed by a small Péclet number, Pe. The perturbations to the equilibrium pair probability owing to the directed motion are small ($O(Pe)$), but they lead to an $O(1)$ correction to the thermodynamic driving forces acting on the particles and thereby affect the average velocity and long-time diffusivity.

We follow the notation and conventions established by Batchelor (1982). We begin with the N-body Smoluchowski equation ensemble averaged to the pair level,

$$\left.\begin{aligned} \frac{\partial p(\boldsymbol{x}_2 \mid \boldsymbol{x}_1)}{\partial t} + \boldsymbol{\nabla}\cdot\boldsymbol{j} &= 0, \\ \boldsymbol{j} &= -\boldsymbol{D}_r\cdot\boldsymbol{\nabla} p(\boldsymbol{x}_2 \mid \boldsymbol{x}_1) + \boldsymbol{V} p(\boldsymbol{x}_2 \mid \boldsymbol{x}_1), \\ P(\boldsymbol{x}_2 \mid \boldsymbol{x}_1) &= n p(\boldsymbol{x}_2 \mid \boldsymbol{x}_1), \end{aligned}\right\} \tag{49}$$

where $\boldsymbol{V}$ is the short-time relative velocity between a pair when one is forced by driving force $\boldsymbol{f}$, the conditional pair probability function replaces the joint probability in (4.2) of Batchelor (1982), the IMPs interact with a hard disk potential, $\boldsymbol{j}$ is flux, and $\boldsymbol{D}_r$ is the relative diffusivity between two isolated IMPs in the suspension.

We make the following definitions,

$$\left.\begin{aligned} \boldsymbol{r} &= \boldsymbol{r}_2 - \boldsymbol{r}_1, \\ \boldsymbol{V} &= \boldsymbol{V}_2 - \boldsymbol{V}_1, \\ \boldsymbol{\nabla} &= \boldsymbol{\nabla}_2 - \boldsymbol{\nabla}_1, \\ \boldsymbol{V} &= \frac{\boldsymbol{f}}{\mu h}\cdot\left[(a_m - b_m)\frac{\boldsymbol{rr}}{r^2} - (c_m - e_m)\left(\boldsymbol{I} - \frac{\boldsymbol{rr}}{r^2}\right)\right], \\ \boldsymbol{D}_r &= \frac{2kT}{\mu h}\left[(a_m - b_m)\frac{\boldsymbol{rr}}{r^2} - (c_m - e_m)\left(\boldsymbol{I} - \frac{\boldsymbol{rr}}{r^2}\right)\right], \end{aligned}\right\} \tag{50}$$

where a_m, b_m, c_m, and e_m are elements of the two-IMP mobility tensor (Bussell *et al.*

1992). The differential equation governs the perturbation to the pair probability distribution, $p(\boldsymbol{x}_2/\boldsymbol{x}_1)$, caused by the convection, $\boldsymbol{V}$, of the tracer relative to neighbouring particles. The boundary conditions to the steady-state equation are that $p(x_2/x_1)\to 1$ as $r\to\infty$, and $\boldsymbol{j}\cdot\boldsymbol{n}\to 0$ as $r\to 2a$. However, it will be seen that the no flux boundary condition at $r=2a$ is satisfied for any non-singular pair probability, p, because the relative diffusivity and relative velocity go to zero as $r\to 2a$. Therefore, the inner boundary condition will be replaced by an analysis based on the form of the differential equation near $r=2a$.

The differential equation simplifies after we substitute the dimensionless variables,

$$\left.\begin{aligned} \boldsymbol{r} &= a\boldsymbol{\rho}, \\ \nabla &= \frac{1}{a}\boldsymbol{\nabla}, \\ \boldsymbol{V} &= V_\infty \bar{\boldsymbol{V}} = \frac{|\boldsymbol{f}|\, a_\infty}{\mu h}\bar{\boldsymbol{V}}, \\ \boldsymbol{D}_{rel} &= D_{rel,\infty}\bar{\boldsymbol{D}} = \frac{2a_\infty kT}{\mu h}\bar{\boldsymbol{D}}, \\ Pe &= \frac{|\boldsymbol{f}|\, a}{2kT}, \end{aligned}\right\} \tag{51}$$

into the equation. Here, a_∞ is the value of a_m as $r\to\infty$. The convective term, $\boldsymbol{V}$, scales like $O(Pe)$, and following Batchelor (1982), we therefore substitute the following expansion for $p(\boldsymbol{x}_2/\boldsymbol{x}_1)$,

$$p(\boldsymbol{x}_2\,|\,\boldsymbol{x}_1) = 1 + Pe\frac{\boldsymbol{f}\cdot\boldsymbol{r}}{|\boldsymbol{f}|\,|\boldsymbol{r}|}Q(\rho). \tag{52}$$

After simplification, equation (49) becomes

$$X\frac{\mathrm{d}^2Q}{\mathrm{d}\rho^2} + Y\frac{\mathrm{d}Q}{\mathrm{d}\rho} + ZQ = W, \tag{53}$$

with

$$\left.\begin{aligned} X &= (a_m - b_m)\rho, \\ Y &= \frac{\mathrm{d}}{\mathrm{d}\rho}[(a_m - b_m)\rho], \\ Z &= -\frac{(c_m - e_m)}{\rho}, \\ W &= -Y + (c_m - e_m). \end{aligned}\right\} \tag{54}$$

The boundary condition as $r\to\infty$ is $Q\to 0$. In order to determine the inner boundary condition, we must consider the asymptotic forms for $a_m - b_m$ and $c_m - e_m$. From the lubrication results for these coefficients (Bussell *et al.* 1992), we find that

$$\left.\begin{aligned} a_m - b_m &= \frac{1}{3\pi}\epsilon^{-\frac{3}{2}}, \\ c_m - e_m &= \frac{1}{2\pi}\epsilon^{-\frac{1}{2}}, \end{aligned}\right\} \tag{55}$$

where $\epsilon = \rho - 2$. Inserting into the expression for j, (49), along with the previous definitions, the inner boundary condition becomes,

$$\left(1+\frac{dQ}{d\rho}\right)O(\epsilon^{\frac{3}{2}}) = 0 \text{ or } \frac{dQ}{d\rho} < O(\epsilon^{-\frac{3}{2}}), \tag{56}$$

which is satisfied if Q is non-singular at $\epsilon = 0$. Seeking a non-singular solution for Q, we substitute a power series expansion for Q about $\epsilon = 0$,

$$Q = {}^0Q + \epsilon({}^1Q) + \epsilon^2({}^2Q), \tag{57}$$

into the differential equation, (53). The leading-order terms are

$${}^1Q - \tfrac{1}{4}({}^0Q) = \frac{dQ}{d\rho} - \tfrac{1}{4}Q = -\tfrac{1}{2}. \tag{58}$$

This condition can be used to start the integration at $\epsilon = 0$. Equation (57) satisfies (56), and based on the condition in (58), Q is well behaved in the region $\epsilon = 0$.

We solve (53) by dividing the domain into inner and tail regions in order to best handle the boundary condition at infinity. Instead of taking the domain as large but finite, we form an asymptotic solution valid at large ρ in order to increase the convergence rate of the solution. In the inner region, we solve the full differential equation using a Runge–Kutta routine. We determine two particular solutions, Q_1 and Q_2. Any linear combination of the two solutions such that $c_1 Q_1 + c_2 Q_2 = 1$ satisfies (53) and (58).

In the large ρ region, all coefficients in the differential equation, (53), are approximated by their values at infinite separation. The values for the zeroth and first derivatives of Q are set equal at the radius of separation, ρ_t, between the two regions. The radius ρ_t is increased until the answer is unaffected by further increases. In the tail region the differential equation takes the form

$$\rho^2\frac{d^2Q}{d\rho^2} + \rho\frac{dQ}{d\rho} + Q = 0, \tag{59}$$

with the solution

$$Q_t = \frac{c_3}{\rho}, \tag{60}$$

which satisfies the boundary condition that $Q \to 0$ as $r \to \infty$. Requiring both Q and $dQ/d\rho$ to be continuous at $\rho = \rho_t$, we determine that the constants c_1, c_2 and c_3, must satisfy the conditions

$$\left.\begin{aligned} c_1 + c_2 &= 1, \\ \frac{c_3}{\rho_t} &= c_1 Q_1 + c_2 Q_2, \\ \frac{-c_3}{\rho_t^2} &= c_1\frac{dQ_1}{d\rho_t} + c_2\frac{dQ_2}{d\rho_t}. \end{aligned}\right\} \tag{61}$$

With the solution for Q and therefore the pair probability $P(x_2|x_1)$, we can determine the contributions of the structure to the long-time diffusion coefficient. The variation in the pair probability leads to equal and opposite Brownian forces acting on

the two particles equal to $-kT\nabla_i(\ln(P(x_i|x_j))$ for $i \neq j$. These forces lead to an additional contribution to the flux and therefore the mobility of the tracer particle given by

$$\Delta U_1 = \boldsymbol{D}_{rel} \cdot \nabla p. \tag{62}$$

Integrating (62) over all particle pairs, we find, after simplification (Batchelor 1982),

$$\langle \Delta U_1 \rangle = -\frac{f}{2\mu h} \int_2^\infty \left[\rho \frac{\mathrm{d}(a_m - b_m)}{\mathrm{d}\rho} + (a_m - b_m + e_m - c_m) \right] Q \, \mathrm{d}\rho. \tag{63}$$

Adding $\langle \Delta U_1 \rangle$ to the results for U from the short-time calculation, taking the absolute value, and normalizing with U_0 gives the result for D_l/D_0. We find that $\langle \Delta U_1 \rangle$ has a value of

$$\frac{\Delta U_1}{U_0} = \frac{-0.07\phi}{\ln(\lambda) - \gamma} = \frac{m_l - m_s}{m_0}. \tag{64}$$

For $\lambda = 250$, this results in the asymptotic form

$$\frac{D_l}{D_0} = 1 - 1.44\phi. \tag{65}$$

There is very little difference between the asymptotic solutions for D_l/D_0 and D_s/D_0. To some extent the similarity in the behaviours of the long- and short-time tracer diffusivities of IMPs could have been anticipated from the nature of the interactions. The hydrodynamic interactions that contribute to the short-time diffusion coefficient occur over separations ranging from $O(a)$ out to $O(\lambda a)$ and they make an $O(\phi)$ contribution to D_s/D_0 and D_l/D_0 as $\lambda \to \infty$. The structure of the pair probability, on the other hand only extends over $O(a)$ separations, and it makes an $O(\phi/\ln(\lambda))$ contribution to $(D_l - D_s)/D_0$ as $\lambda \to 0$. Thus, if $\ln(\lambda)$ is sufficiently large the short- and long-time diffusivities must have similar values. However, the small magnitude of the numerical coefficient (-0.07) in the numerator of (64) could not have been anticipated from this argument and this value is even smaller than the corresponding coefficient in the calculation for spheres (Batchelor & Wen 1982).

We can also compare our results for the asymptotic value for D_l/D_0 to theories which neglect hydrodynamics. The result for D_l/D_0 for IMPs interacting with hard-core interactions and neglecting hydrodynamic interactions is $D_l/D_0 = 1 - 2\phi$ (Abney *et al.* 1989*a*). Evidently, hydrodynamic interactions decrease the effect of hard-core interactions as $\phi \to 0$.

4. Gradient diffusion

The calculation of gradient diffusion coefficients closely follows the calculation for tracer diffusion coefficients. The difference between the calculations is that all of the particles in the gradient diffusion problem experience the thermodynamic driving force, whereas only the tracer particle experiences a driving force in the tracer diffusion problem. In order to make the analysis of the problem tractable, we must assume that the concentration field obeys the relation $L|\nabla \ln n| \ll 1$ (Batchelor 1976). This guarantees that all particles in an L^2 neighbourhood experience the same thermodynamic driving force. A simplification arises in the calculation of gradient diffusion coefficients in monodisperse suspensions since no relative motions between IMPs occur

when considering interactions at the pair-level. Thus, we do not need to calculate perturbation distribution functions in order to calculate D_g.

Until we proceed to the level involving two-particle interactions, the gradient diffusion problem is indistinguishable from the tracer problem. At the level at which a single particle is experiencing a thermodynamic force independent of other particles, its velocity is $\boldsymbol{U}_0$ given by (31). Recalling our discussion of the method of reflections, three terms require renormalization at the next level at which two-particle interactions are important. The effective medium must reflect the pair-wise divergent contributions which arise in the tracer problem along with the force and quadrupole terms introduced by the neighbouring proteins in response to the thermodynamic force. As a consequence, the effective medium differs for a particle undergoing gradient diffusion from one undergoing tracer diffusion.

The effective viscosity again enters the renormalization for the response of neighbouring particles to the flow field generated by a central protein. We follow the work of Batchelor (1972) and Hinch (1977) to renormalize the remaining terms. Originally, this renormalization was considered in the context of sedimenting particles (Batchelor 1972) and only later was it extended to the gradient diffusion problem (Batchelor 1976).

The strengths of the divergences arising from the force and quadrupole terms are given by (29), the velocity disturbance caused by a forced particle. The distribution of forces for $r > 2a$ is $(\boldsymbol{f}_p/V_p)\, g\phi$, where each particle has a force strength $\boldsymbol{f}_p$ and a volume V_p. In the sedimentation problem, it can be thought of as an increase in the density of the bulk fluid. Thus, the renormalized form of (20) for the gradient diffusion problem is, for $|\boldsymbol{x}-\boldsymbol{x}_1| > 1$,

$$
\begin{aligned}
&-\nabla\langle p\rangle(\boldsymbol{x}\,|\,\boldsymbol{x}_1)+\nabla\cdot(2\mu^*\langle \boldsymbol{E}\rangle(\boldsymbol{x}\,|\,\boldsymbol{x}_1))\\
&\quad+\int_{|\boldsymbol{x}_1-\boldsymbol{x}_2|\geqslant 2a}\left[\frac{g(\boldsymbol{x}\,|\,\boldsymbol{x}_1)\boldsymbol{f}_p\phi}{V_p}(1+\tfrac{1}{4}a^2\nabla_2^2)\,\delta(\boldsymbol{x}-\boldsymbol{x}_2)\right]\mathrm{d}V_2+\frac{2}{h}\langle\boldsymbol{\sigma}\rangle(\boldsymbol{x}\,|\,\boldsymbol{x}_1)\\
&=-\nabla\cdot\int_{|\boldsymbol{x}_1-\boldsymbol{x}_2|\geqslant 2a}\Big[\langle \boldsymbol{T}^p\rangle(\boldsymbol{x}\,|\,\boldsymbol{x}_1,\boldsymbol{x}_2)\,P(\boldsymbol{x}_2\,|\,\boldsymbol{x}_1)-4g(\boldsymbol{x}\,|\,\boldsymbol{x}_1)\,\phi\mu\langle \boldsymbol{E}\rangle(\boldsymbol{x}_2\,|\,\boldsymbol{x}_1)\,\delta(\boldsymbol{x}-\boldsymbol{x}_2)\\
&\quad-\frac{\boldsymbol{f}_p\,g(\boldsymbol{x}\,|\,\boldsymbol{x}_1)\,\phi}{V_p}(1+\tfrac{1}{4}a^2\nabla_2^2)\,\delta(\boldsymbol{x}-\boldsymbol{x}_2)\Big]\mathrm{d}V_2.
\end{aligned}
\tag{66}
$$

The new terms relative to the renormalized equation for the tracer particle, (35), are the force and quadrupole terms, given by (33), which arise from neighbouring particles experiencing the thermodynamic force. An essential feature of the renormalization in gradient diffusion and sedimentation problems is that the uniform body force $\phi\boldsymbol{f}_p/V_p$ exerted by the particles far from the fixed particle does not drive a fluid velocity but rather only changes the average pressure gradient (Hinch 1977). In the case of a sedimenting suspension of spheres this uniform body force can be eliminated from the average momentum equation by adopting a reduced pressure based on the average density of the suspension rather than the fluid density. In the present application to a suspension of particles within a membrane experiencing a common thermodynamic driving force, this uniform force distribution produces a mean pressure gradient within the membrane but does not drive a fluid flow either within the membrane or in the surrounding aqueous phases. In addition, the uniform force distribution in the membrane does not affect the pressure in the aqueous phases as may be seen from (66), (24) and (27).

To understand this point physically, it is useful to contrast the present case of a planar array of particles embedded in a lipid bilayer surrounded by two aqueous phases to a planar array of spheres within a single three-dimensional fluid. In the latter case, the body force exerted by the spheres and the resulting pressure gradient would drive fluid out of the layer occupied by the spheres, thus driving a fluid flow that would greatly accelerate the translation of the spheres. However, strong thermodynamic forces keep the lipid molecules within the plane of the membrane and therefore the pressure gradient within the membrane and the pressure imbalance between the membrane and the aqueous phase does not drive a fluid flow.

The solution to (66) follows a progression similar to the solution of (35). If the velocity is expanded in a Taylor series, the equation for the zeroth-order velocity includes only the two non-integral terms on the left-hand side of (66). It is the same as the zeroth-order equation for the tracer velocity, (43), which we call ${}^1\boldsymbol{U}$. We use the asymptotic form for ${}^1\boldsymbol{U}$ as $\phi \to 0$, (44), in order not to exceed the $O(\phi)$ precision of the results.

The governing equation for the $O(\phi)$ correction is similar to (38) but involves all the integral terms in (66). Because of the linearity of (38) and the analogous equation for the first-order solution of (66), the various contributions to the remainder for the velocity of particle 1 can be obtained individually using the two-dimensional Oseen–Burgers tensor. The most convenient method to calculate the remainder involves five separate additional contributions to the tracer velocity labelled ${}^2\boldsymbol{U}-{}^6\boldsymbol{U}$ which we describe in turn. Therefore, the final result for the velocity of a central IMP in response to a force on all IMPs in an L^2 neighbourhood is the sum of the six contributions, ${}^1\boldsymbol{U}-{}^6\boldsymbol{U}$.

The force distribution of $(\boldsymbol{f}_p/V_p)g\phi$ in $r > 2a$ is most easily calculated by decomposing it into three terms – a uniform distribution, $(\boldsymbol{f}_p/V_p)\phi$, everywhere, a distribution of $-(\boldsymbol{f}_p/V_p)\phi$ in $r < 2a$, and a distribution of $(g-1)(\boldsymbol{f}_p/V_p)\phi$ for $2a < r < R_{trunc}$. The force distribution everywhere produces an $O(\phi)$ correction to the pressure gradient, but no changes to the velocity of the central particle as discussed above. The force distribution of $-(\boldsymbol{f}_p/V_p)\phi$ in $0 < r < a$ alters the effective force on the central particle and induces a disturbance to its velocity, ${}^2\boldsymbol{U}$, equal to $-\boldsymbol{U}_0\phi$, where $\boldsymbol{U}_0$ is the velocity of an isolated protein given by (31).

Calculation of the velocity resulting from the force distribution in $a < r < 2a$ is more involved and makes use of the Faxén law, (29). The force on the disk, $\boldsymbol{f}$, is zero, and $\boldsymbol{v}_\infty$ is the flow field produced by the force distribution. Substituting the expression for $\boldsymbol{v}_\infty$, (32), into the Faxén law, we find a disturbance particle velocity

$$ {}^3\boldsymbol{U} = (1+\tfrac{1}{4}a^2\nabla^2)\int_{|\boldsymbol{x}_2-\boldsymbol{x}_1|=a}^{|\boldsymbol{x}_2-\boldsymbol{x}_1|=2a} (\boldsymbol{f}^{(n)}m+\boldsymbol{f}^{(n)}\cdot\boldsymbol{J}(\boldsymbol{x}-\boldsymbol{y}^{(n)}))\,P(\boldsymbol{x}_2\,|\,\boldsymbol{x}_1)\,\mathrm{d}V_y, \tag{67} $$

where $\boldsymbol{f}^{(n)} = -(\boldsymbol{f}_p/V_p)$. The integral has the value

$$ {}^3\boldsymbol{U} = \boldsymbol{U}_0\phi\left[-4+\frac{4\ln(2)-1.5}{\ln(\lambda)-\gamma}\right]. \tag{68} $$

The calculation of the velocity resulting from the force distribution in $2a < r < R_{trunc}$, ${}^4\boldsymbol{U}$, is identical to the calculation of ${}^3\boldsymbol{U}$, except it must be performed numerically. Obviously, in the limit as $\phi \to 0$, the contribution from this term is 0 because $g = 1$ for $r > 2a$.

For convenience, we utilize a slightly different approach to evaluate the effect of the quadrupoles. The presence of the Laplacian operator as part of the quadrupole term

in (66) enables us to transform the volume integral for this contribution to a surface integral. After inversion and transformation, the expression for the quadrupole contribution is

$$^5U = (1+\tfrac{1}{4}a^2\nabla^2)\frac{a^2}{4}\frac{N}{V}\Big\{\int_{|x_2-x_1|=2a} \boldsymbol{f}^{(n)}\cdot(\boldsymbol{n}\cdot\nabla\boldsymbol{J}(\boldsymbol{y}^{(n)}-\boldsymbol{x}_1))\,g(\boldsymbol{x}_2=\boldsymbol{y}^{(n)}\,|\,\boldsymbol{x}_1)\,\mathrm{d}S_y$$

$$+\int_{|x_2-x_1|>2a} \boldsymbol{f}^{(n)}\cdot(g(\boldsymbol{x}_2=\boldsymbol{y}^{(n)}\,|\,\boldsymbol{x}_1)-1)\,\nabla^2\boldsymbol{J}(\boldsymbol{y}^{(n)}-\boldsymbol{x}_1)\,\mathrm{d}V_y\Big\}, \quad (69)$$

where $\boldsymbol{n}$ is the unit outward normal relative to particle 1. There is a similar surface integral for $|\boldsymbol{y}^{(n)}-\boldsymbol{x}_1|$ at ∞, but its value is zero because the boundary conditions stipulate that gradients of the velocity decay to zero as $|\boldsymbol{y}^{(n)}-\boldsymbol{x}_1|\to\infty$. The result for the integral at $r=2a$ and any g for $r>2a$ is

$$^5U = \tfrac{1}{2}U_0\,\phi[\ln(\lambda)-\gamma]^{-1}. \quad (70)$$

It turns out that the volume integral in (69) makes no contribution when $g \neq 1$ for $r>2a$ (Batchelor 1972).

The contribution to the velocity resulting from the integrals on the right-hand side of (66), ^6U, involves the solution to the isolated two-particle problem. The expression for the remainder term is

$$\text{remainder} = \int_{|x_1-x_2|\geqslant 2a} [\boldsymbol{U}_2 - 4\pi\mu a^2\boldsymbol{E}(\boldsymbol{x}_2\,|\,\boldsymbol{x}_1):\nabla\boldsymbol{J}(\boldsymbol{x}_2-\boldsymbol{x}_1)$$

$$-(1+\tfrac{1}{4}a^2\nabla^2)\,\boldsymbol{U}_1]\,P(\boldsymbol{x}_2\,|\,\boldsymbol{x}_1)\,\mathrm{d}V_2, \quad (71)$$

where

$$\boldsymbol{U}_2 = \frac{\boldsymbol{f}}{\mu h}\cdot\left(\frac{(a_m+b_m)\,\boldsymbol{xx}}{r^2}+(c_m+e_m)\left(\boldsymbol{I}-\frac{\boldsymbol{xx}}{r^2}\right)\right), \quad (72)$$

and $\boldsymbol{U}_1$ is the velocity of the central protein as given by the Faxén law which results from the force and quadrupole distribution. For the case $g=1$ for $r>2a$,

$$^6U = \frac{0.37\phi}{\ln(\lambda)-\gamma}. \quad (73)$$

If $g \neq 1$ for $r>2a$, ^6U is a function of g and therefore changes with ϕ. The integral in (71) converges like

$$\int {}^3U r\,\mathrm{d}r = \int O(r^{-4})\,r\,\mathrm{d}r = O(r^{-3}\,\mathrm{d}r).$$

Although the right-hand side integral for the gradient problem does not converge as quickly as the one for the tracer problem, we are still justified to consider interactions only in $r \ll \lambda a$ because λ is $O(100)$.

We must now sum the six contributions to the velocity of the central particle. The result is

$$\boldsymbol{U} = \left\{1+\left[-7+\frac{1}{\ln(\lambda)-\gamma}(6\ln(2)+\tfrac{7}{16})\right]\phi\right\}\boldsymbol{U}_0 + {}^4\boldsymbol{U} + {}^6\boldsymbol{U} = m_g\boldsymbol{f}^*, \quad (74)$$

where we solve for $^4\boldsymbol{U}$ and $^6\boldsymbol{U}$ numerically at non-zero ϕ, and their results are in table 1. The result for m_g in (74) is related to D_g by (10).

	${}^4U/U_0 = A+B$		
ϕ	A	$B(\ln(\lambda)-\gamma)$	$({}^6U/U_0)(\ln(\lambda)-\gamma)$
0	0	0	0.37ϕ
0.1	0.014	0.032	0.038
0.2	0.052	0.15	0.080
0.3	0.26	0.026	0.12
0.4	0.62	−0.31	0.17
0.453	0.83	−0.49	0.20
0.5	1.0	−0.65	0.22
0.6	1.3	−0.61	0.26

TABLE 1. The intermediates ${}^4U$ and ${}^6U$ which contribute to the solution for m_g and, thus, D_g

In order to complete the calculation for D_g, we must calculate the thermodynamic force. Batchelor (1976) derived an expression for D_g in terms of the thermodynamic force and the hydrodynamic mobility. He found that

$$D_g \boldsymbol{I} = m_g \frac{\phi}{1-\phi}\left(\frac{\partial\tilde{\mu}}{\partial\phi}\right)_{p,T} \boldsymbol{I}, \tag{75}$$

where p is pressure, T is absolute temperature, and $\tilde{\mu}$ is the chemical potential. The expression involving $\tilde{\mu}$ is expanded in the series,

$$\phi\left(\frac{\partial\tilde{\mu}}{\partial\phi}\right)_{p,T} = kT(1-\phi)\left(1-\sum_{j=1}^{\infty} j\beta_j\phi^j\right), \tag{76}$$

so that the solution for D_g to $O(\phi)$ involves the terms in (76) up to and including $j=1$ for which $\beta_1 = -4$ for disks (Abney *et al.* 1989*b*). The combination of (76), (75) and (74) yields the results for D_g. The low ϕ asymptote is

$$\frac{D_g}{D_0} = 1+\left[-7+\frac{6\ln(2)+\frac{7}{16}+0.37}{\ln(\lambda)-\gamma}\right]\phi+O(\phi^2). \tag{77}$$

For $\lambda = 250$ it is

$$\frac{D_g}{D_0} = 1-6.0\phi+O(\phi^2). \tag{78}$$

Equations (77) and (78) give the rigorous results for the gradient diffusivity of IMPs in the limit of small area fraction and these are the primary results of this section. We can compare our results to previous theoretical calculations of D_g which ignore hydrodynamic interactions (Abney *et al.* 1989*b*). Their results for hard disks show a monotonic increase for D_g, and the low ϕ asymptote is directly related to the thermodynamic force and has the value $1+4\phi$. This contrasts drastically with the hydrodynamically consistent result that as $\phi\to 0$, $D_g\to 1-6.0\phi$ for $\lambda = 250$. The mitigation of D_g caused by decreased mobilities overpowers the enhancement caused by the thermodynamic forces. The analogous result for spheres for which $D_g/D_0 = 1+1.45\phi$ contrasts with (78) because in the three-dimensional case the thermodynamic effect is larger than the hydrodynamic effect and D_g/D_0 is greater than 1 in the limit $\phi\to 0$ (Batchelor 1983).

In addition to the asymptotic results for small area fraction, we have computed the gradient diffusivity at higher area fractions based on a pairwise approximation of the renormalized hydrodynamic interactions, but including the structure of the pair

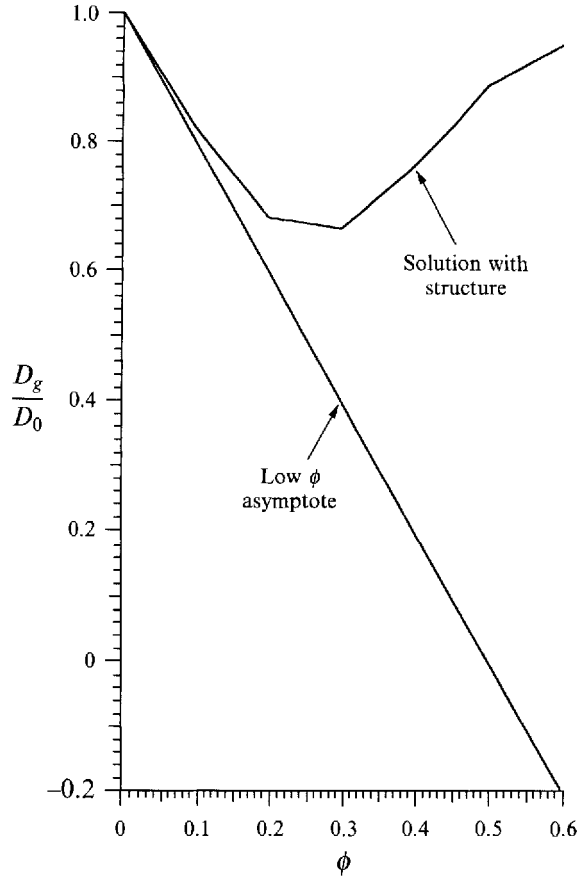

FIGURE 4. Two solutions for the normalized gradient diffusion coefficient, D_g/D_0, a low ϕ asymptote and a solution that incorporates membrane structure at high ϕ. The roughness of the curve for the solution with structure is a result of the small number of data points used to generate it.

probability $g(\phi, r)$ for an equilibrium hard-disk distribution. This approximation is analogous to one given by Glendinning & Russel (1982) for suspensions of spheres. The calculation with structure along with the rigorous low ϕ asymptote are plotted in figure 4. The structure has a much larger effect on the gradient diffusivity than it did on the short-time tracer diffusivity. The structure of the pair probability leads to a gradient diffusion coefficient that is positive for all values of ϕ unlike the low ϕ asymptote. However, these results are only presented as a tentative first step toward predicting the gradient diffusivity of IMPs at higher area fractions. The comparable approximation for spherical particles has not proved very successful as it gives negative values of D_g for volume fractions greater than about 0.27 (Glendinning & Russel 1982) and does not agree with numerical simulations (Brady & Durlofsky 1988). A proper assessment of the validity of the pairwise additive approximation in the present case awaits numerical simulations for IMPs.

5. Conclusions

We have calculated the effect of hydrodynamic interactions on the short- and long-time tracer diffusivity and gradient diffusivity of IMPs by considering their two-body hydrodynamic interactions. We have ensemble averaged the N-body Stokes equations

and then renormalized and solved the resulting one-particle conditionally averaged equations. The results are rigorously valid in the limit $\phi \to 0$.

The results for D_s/D_0 are plotted in figure 3. The low ϕ asymptote given by (45) has $O(\phi^2)$ errors. It is always numerically smaller than the effective medium approximation, given in (43), which uses $g = 1$ for $r > 2a$. Incorporating non-uniform g into the effective medium approximation has little influence on the results for D_s. Hydrodynamic interactions are the sole determinant for D_s, and it has only recently been possible to calculate D_s to $O(\phi)$, since the hydrodynamic interactions between proteins were only recently calculated (Bussell *et al.* 1992). Experiments using spectroscopic techniques such as electron spin resonance and nuclear magnetic resonance, which have temporal resolutions of 10^{-8} and 10^{-5} s, respectively (Gennis 1989), are needed in order to measure the $O(10^{-5}$ s) and faster timescale motions which contribute to D_s.

In the limit $\phi \to 0$, differences between m_l and m_s, given by (57), are relatively small so that D_l is nearly the same as D_s. This result contrasts with results for spheres (Batchelor 1982). Furthermore, values of D_l/D_0 given by (65) decrease with increasing ϕ slower than results based solely on hard-core interactions (Abney *et al.* 1989*a*). However, at higher area fractions there may be significant differences between D_l and D_s because of strong excluded area effects. Comparisons of the theoretical results with experimental data on the diffusion of proteins in lipid bilayers will require an extension of this theory to higher area fractions.

Lastly, the results for D_g/D_0 are plotted in figure 4. The low ϕ asymptote is given by (78), and D_g/D_0 decreases monotonically as ϕ increases. The pairwise additive approximation incorporating the structure of the pair probability deviates strongly from the low ϕ asymptote. It displays a minimum at $\phi \sim 0.3$ and approaches 1 at high ϕ. This contrasts both with the results for spheres (Batchelor 1983) for which $D_g/D_0 > 1$ at low ϕ and the results for D_g/D_0 for hard-core disks neglecting hydrodynamics for which D_g/D_0 is also greater than 1 (Abney *et al.* 1989*b*). For both the tracer and gradient diffusion coefficients, the most important results of the paper are the rigorously valid small area fraction asymptotes (45), (65) and (78). The results given in figures 3 and 4 simply represent a first attempt to approximate the short-time tracer diffusivity and gradient diffusivities at higher area fractions and more reliable results for high area fraction will require Stokesian dynamic numerical simulations.

We would like to thank Travis Dodd for his help with the Monte-Carlo simulations for radial distribution functions. This work was supported by the National Science Foundation in the form of a Creativity Award (EID-8710373) to S.J.B. and Presidential Young Investigator Awards to D.L.K. (CTS-8857565) and to D.A.H. (BCS-8958632).

REFERENCES

ABNEY, J. R., SCALETTAR, B. A. & OWICKI, J. C. 1989*a* Self diffusion of interacting membrane proteins. *Biophys. J.* **55**, 817–833.

ABNEY, J. R., SCALETTAR, B. A. & OWICKI, J. C. 1989*b* Mutual diffusion of interacting membrane proteins. *Biophys. J.* **56**, 315–326.

AGUIRRE, J. L. & MURPHY, T. J. 1973 Brownian motion of N interacting particles. II. Hydrodynamical evaluation of the diffusion tensor matrix. *J. Chem. Phys.* **59**, 1833–1840.

BATCHELOR, G. K. 1972 Sedimentation in a dilute dispersion of spheres. *J. Fluid Mech.* **52**, 245–268.

BATCHELOR, G. K. 1976 Brownian diffusion of particles with hydrodynamic interactions. *J. Fluid Mech.* **74**, 1–29.

BATCHELOR, G. K. 1982 Sedimentation in a dilute polydisperse system of interacting spheres. Part 1. General theory. *J. Fluid Mech.* **119**, 379–408.

BATCHELOR, G. K. 1983 Diffusion in a dilute polydisperse system of interacting spheres. *J. Fluid Mech.* **131**, 155–175.

BATCHELOR, G. K. & WEN, C.-S. 1982 Sedimentation in a dilute polydisperse system of interacting spheres. Part 2. Numerical results. *J. Fluid Mech.* **124**, 495–528.

BRADY, J. F. 1984 The Einstein viscosity correction in *n* dimensions. *Intl J. Multiphase Flow* **10**, 113–114.

BRADY, J. F. & BOSSIS, G. 1988 Stokesian dynamics. *Ann. Rev. Fluid Mech.* **20**, 111–157.

BRADY, J. F. & DURLOFSKY, L. J. 1988 The sedimentation rate of disordered suspensions. *Phys. Fluids* **31**, 717–727.

BUSSELL, S. J., KOCH, D. L. & HAMMER, D. A. 1992 The resistivity and mobility functions for a model system of two equal-sized proteins in a lipid bilayer. *J. Fluid Mech.* **243**, 679–697.

CHAZOTTE, B. & HACKENBROCK, C. R. 1988 The multicollisional, obstructed, long-range diffusional nature of mitochondrial electron transport. *J. Biol. Chem.* **263**, 14359–14367.

CHAE, D. G., REE, F. H. & REE, T. 1969 Radial distribution functions and equation of state of the hard-disk fluid. *J. Chem. Phys.* **50**, 1581–1589.

GENNIS, R. B. 1989 *Biomembranes: Molecular Structure and Function.* Springer.

GLENDINNING, A. B. & RUSSEL, W. B. 1982 A pairwise additive description of sedimentation and diffusion in concentrated suspensions of hard spheres. *J. Colloid Interface Sci.* **89**, 124–142.

HINCH, E. J. 1977 An averaged-equation approach to particle interactions in a fluid suspension. *J. Fluid Mech.* **83**, 695–720.

KIM, S. & KARRILA, S. J. 1991 *Microhydrodynamics: Principles and Selected Applications.* Butterworth–Heinemann.

METROPOLIS, N., ROSENBLUTH, A., ROSENBLUTH, M., TELLER, A. & TELLER, E. 1953 Equations of state calculations by fast computing machines. *J. Chem. Phys.* **21**, 1087–1092.

PETERS, R. & CHERRY, R. J. 1982 Lateral and rotational diffusion of bacteriorhodopsin in lipid bilayers: experimental test of the Saffman–Delbruck equations. *Proc. Natl Acad. Sci. USA* **79**, 4317–4321.

PHILLIPS, R. J., BRADY, J. F. & BOSSIS, G. 1988 Hydrodynamic transport properties of hard-sphere dispersions. I. Suspensions of freely mobile particles. *Phys. Fluids* **31**, 3462–3472.

QIAN, H., SHEETZ, M. P. & ELSON, E. L. 1991 Single particle tracking: analysis of diffusion and flow in two-dimensional systems. *Biophys. J.* **60**, 910–921.

RALLISON, J. M. 1988 Brownian diffusion in concentrated suspensions of interacting particles. *J. Fluid Mech.* **186**, 471–500.

SAFFMAN, P. G. 1976 Brownian motion in thin sheets of viscous fluid. *J. Fluid Mech.* **73**, 593–602.

SAXTON, M. J. 1987 Lateral diffusion in an archipelago: the effect of mobile obstacles. *Biophys. J.* **52**, 989–997.